- Technical Paper -

MULTI-LAYERED MICROPLANE MODEL FOR STRAIN HARDENING CEMENT-BASED COMPOSITES

Umbreen-Us-Sahar[*1], Tatsuya TSUBAKI[*2]

ABSTRACT

The tensile properties of strain hardening cementitious composites are modelled by using multi-layer microplane model with multi-layered microplane structure. In the simulation to verify the validity of the present model, the statistical variation of material properties due to spatial distribution of short randomly distributed fibers are considered. The total crack widths and stress-strain relationship are examined for uniaxial direct tensile loading along with crack distribution, spacing and number of cracks. The analytical results are compared with experimental data. The uniaxial compression behavior is also verified. A good agreement is found in analytical and experimental values.

Keywords: multiple cracking, SHCC, microplane model

1. INTRODUCTION

Strain hardening cementitious composites is the material which exhibits strain hardening, quasi-ductile behavior due to bridging of fine multiple cracks by short, randomly distributed polymer fibers as shown in Fig.1. The strain hardening is followed by the phenomenon of increased tensile load with increased overall elongation. The favorable mechanical properties of this material offer many possible applications in new and old structures as well as in the strengthening and repair of structural elements made of reinforced concrete or other traditional materials [1].

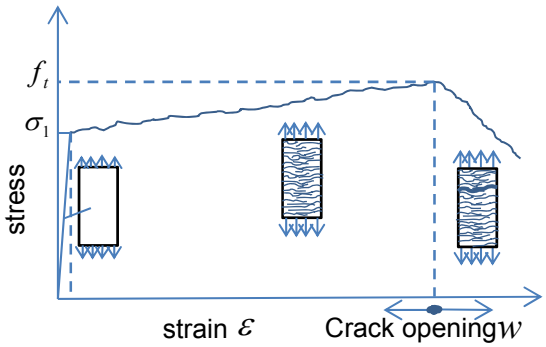

Fig.1 Multiple cracking system in SHCC

Several research projects have proposed different modelling approaches for SHCC subjected to tensile loading. Han et al.[2] and Vorel and Boshoff [3] introduced the constitutive relations for SHCC based on the reproduction of experimental results obtained from the test on bulk SHCC specimen. The derived formulas are adequate for the use in structural analysis. Much less focus has been given on the effect on mechanical properties of SHCC based on statistical variation in material properties and still it is needed to explain the modelling of material micromechanical behavior based on statistical variation that can be implemented for not only uniaxial tension and compression but also for biaxial and multiaxial behavior of SHCC. Besides this more study is very essential to model crack width and number of cracks in a multiple cracking system.

This model reflects the fact that the fiber volume fraction V_f in reality varies between individual crack planes (mainly due to material processing in fresh state). This implies that V_f is a random variable. This study presents the multilayer model that can predict stress-strain relationship under uniaxial tensile loading (after combining with microplane model) as well as the uniaxial compression behavior. Namely, this study presents explicitly prediction for total crack width as recursive form of expressions.

In microplane model, the constitutive properties are characterized separately on planes of various orientations within the material, called the microplanes. Kinematic constraint is used on these microplanes, i.e., the total strain vector on each microplane (crack) is assumed to be resolved component of the macroscopic strain tensor while the fibers are assumed to be directed to normal to each microplane. The state of each microplane is described by normal deviatoric and volumetric strain and by shear strain (further split into two orthogonal components) [4].

2. MULTI-LAYERED MICROPLANE MODEL

Multiple cracking behavior can be modelled by expressing total strain by summation of strains in the uncracked part and those in the cracked part [5].

$$d\varepsilon = \sum_{i=1}^{N_C} (\varepsilon_i) \qquad (1)$$

*1 Graduate Program, Graduate School of Urban Innovation, Yokohama National University, JCI Student Member
*2 Professor, Faculty of Urban Innovation, Graduate School, Yokohama National University, JCI Member

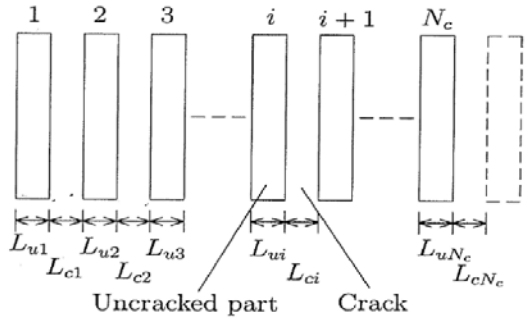

Fig .2 Multiple cracking system in SHCC

$$d\varepsilon_i = d\varepsilon_{cri} + d\varepsilon_{ui} \qquad (2)$$

where N_C is the number of cracks, $d\varepsilon_{cri}$ and $d\varepsilon_{ui}$ are the strain increments for cracked and uncracked part respectively. The multiple cracking system is shown in Fig.2 where L_{ui} and L_{ci} are the lengths of uncracked part and cracked part at i -th crack respectively. The total strain, then, can be obtained by the substitution of the equations for strain increments of uncracked and cracked parts in Eq.2.

2.1 Material condition before cracking

The Fig.3 shows the material condition when stress σ is applied to SHCC specimen (with original length L_0 and length after elongation is L). The applied stress is less than the tensile strength before cracking. Therefore, the elastic modulus of SHCC (by composite law) E and tensile strength (by empirical relationship) f_t can be expressed as

$$E = V_m E_m + V_f E_f = (1 - V_f) E_m + V_f E_f \qquad (3)$$

$$f_t = V_m f_{tm} + V_f f_{tf} = (1 - V_f) f_{tm} + V_f f_{tf} \qquad (4)$$

Where V_f is local fiber volume fraction, V_m is volume fraction of matrix, E_f is elastic modulus of fiber, E_m is elastic modulus of matrix, f_{tm} is tensile strength of matrix, f_{tf} is tensile strength of fiber. When $\sigma = E\varepsilon < f_t$ then $\varepsilon = \Delta u / L_0$ where σ is applied tensile stress in uncracked part, Δu is change in length after applying stress and ε is strain in uncracked part.

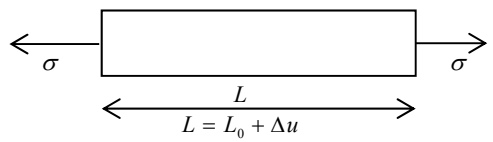

Fig.3 Material condition before cracking

2.2 Assumptions

The following assumptions are used for the multi-layered model based on multiple cracking system.

(1) $P_i = P_{fi}$, where P_i and P_{fi} are the loads in i -th uncracked and cracked part respectively.

(2) $\sigma_{fi} < \sigma_{f0}$, where σ_{fi} is the fiber pullout stress in bridging fibers at i -th crack and σ_{f0} is the maximum bridging stress of fibers acting on a microplane with normal vector **n** as shown in Fig 4(a),(b).

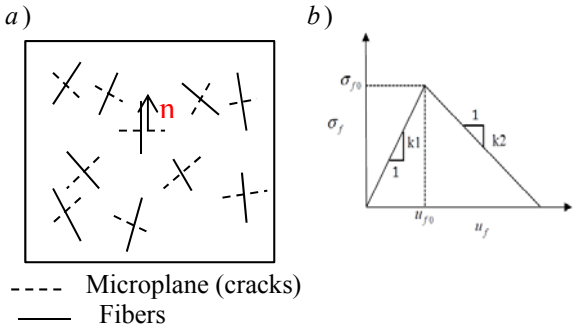

Fig.4 a) Fibers and microplanes b) The fiber pullout force~displacement relationship

(3)Bilinear relationship for the bridging (pullout) stress-fiber pullout displacement is assumed Fig.4 (b).

2.3 Numerical Model

Due to spatial distribution of short fibers, the material properties have a certain amount of statistical variation concluding that V_f is the only independent parameter. The statistical distribution of the fiber volume fraction V_f is assumed to follow the uniform distribution with mean m_{V_f}, the standard deviation σ_{V_f} and the coefficient of variation $w_{V_f} = \sigma_{V_f} / m_{V_f}$. It is assumed that cracking sequence is in the increasing order of tensile strength of SHCC.

Now at first crack $\sigma_1 = f_{t1}$ where σ_1 and f_{t1} are the stress applied and the tensile strength of material at first crack respectively as in Fig.5. To apply assumption (1), the following relations are considered.

$$P = \sigma . A \,(A = bh) \qquad (5)$$

$$P_f = \sigma_f . A_f \,(A_f = N_f . A_{f0}) \qquad (6)$$

where P is load passing through uncracked part, A is the cross sectional area of uncracked part with width b and height h , P_f is the load passing through bridging fibers, A_f is the area of fibers, N_f is the number of bridging fibers, $A_{f0}$is cross sectional area of single fiber, σ_f is bridging stress of fiber (Addition of 1,2,3...i..N_C in the subscripts represents the condition corresponding to given number of crack). Therefore, considering assumption (1),

$$P_{f1} = P, \qquad \sigma_f A_{f1} = f_{t1} A \qquad (7)$$

$$\sigma_f = \frac{A}{A_{f1}} f_{t1} \qquad (8)$$

Considering assumption (3),

$$u_{f1} = \frac{\sigma_f}{k_{f1}} = \frac{A . f_{t1}}{A_{f1} k_{f1}} = (w_1)^I \qquad (9)$$

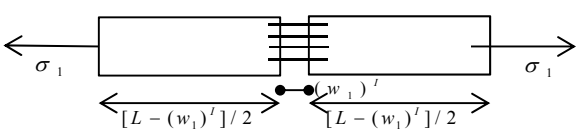

Fig.5 Material condition after first crack

where u_{f1} is the fiber pullout displacement at first crack, k_{f1} is the stiffness of fiber at first crack and $(w_1)^I$ is the individual crack width of the first crack. Hence total strain of cracked part after first crack is ε_{cr1} that can be evaluated as

$$\varepsilon_{cr1} = \frac{(w_1)^I}{L_0} \tag{10}$$

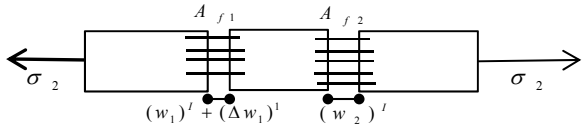

Fig.6 Material condition after 2nd crack

For 2nd crack, the condition is $f_{t1} < f_{t2}$ (due to statistical variation of tensile strength) see Fig.6. Hence when $\sigma_2 = f_{t2}$, 2nd crack will appear. The individual width at 2nd crack level is $(w_2)^I$ that can be evaluated as

$$(w_2)^I = \frac{Af_{t2}}{A_{f2}k_{f2}} \tag{11}$$

where f_{t2} is the increased tensile strength at 2nd crack corresponding to increased local fiber volume. Meanwhile, the first crack width increases due to difference of load/stress at 2nd crack stage and 1st crack stage.

$$(\Delta w_1)^1 = \frac{P_{f2} - P_{f1}}{A_{f1}k_{f1}} = \frac{\Delta P_{f(1-2)}}{A_{f1}k_{f1}} \tag{12}$$

where P_{f1} and $P_{f2}$are the load at first crack stage and 2nd crack stage respectively, $\Delta P_{f(1-2)}$ is the difference of load at 1st and 2nd crack stage. and $(\Delta w_1)^1$ is the increase in first crack width due to difference of loading. Hence total crack width at 2nd crack is $(w_2)^T$ i.e,

$$(w_2)^T = (w_2)^I + (w_1)^I + (\Delta w_1)^1 \tag{13}$$

$$\varepsilon_{cr2} = \frac{(w_2)^T}{L_0} \tag{14}$$

where ε_{cr2} is the strain at 2nd crack stage and $L_0$is the original length of specimen and superscript 'I' with w_i represents the individual crack width and superscript 'T' represents the total crack width at i-th crack stage while superscript $1,2,3...i..N_C$ with Δw_i represents the increase of crack width due to increase in load from i to $i+1$.

Following the same sequence, the equation to calculate displacement at i-th crack stage for N_C number of cracks can be expressed as follows.

$$(w_i)^T = \left[\sum_{i=1}^{N_c} (w_i)^I + g \right] \tag{15}$$

where

$$g = \sum_{i=1}^{N_C} \left(\frac{P_{fi} - P_{f(i-1)}}{k_{f(i-1)} \cdot A_{f(i-1)}} \right) + \sum_{i=1}^{N_C} \left(\frac{P_{fi} - P_{f(i-1)}}{k_{f(i-2)} \cdot A_{f(i-2)}} \right) + \ldots + \sum_{i=1}^{N_C} \left(\frac{P_{fi} - P_{f(i-1)}}{k_{f(i)-(i-N_C)} \cdot A_{f(i)-(i-N_C)}} \right) \tag{16}$$

and $(w_i)^T$is the total crack width at i-th crack stage, $(w_i)^I$ is the individual crack width at i-th crack stage.Hence the strain at i-th stage of cracks for cracked part is ε_{cri} that can be calculated in terms of stiffness of fiber by using Eq.17

$$\varepsilon_{cri} = \frac{(w_i)^T}{L_0} \tag{17}$$

2.4 Implementation of multi-layered model in microplane model

The incremental macroscopic stress-strain relation as per microplane model is given as

$$\Delta\sigma_{ij} = C_{ijrs}(\Delta\varepsilon_{rs} - \Delta\varepsilon_{rs}^{sh} - \Delta\varepsilon_{rs}^{T}) - \Delta\sigma_{ij}^{cr} - \Delta\sigma_{ij}'' \tag{18}$$

where $\Delta\sigma_{ij}$ and $\Delta\varepsilon_{rs}$ are the macroscopic stress and strain increments, $\Delta\varepsilon_{rs}^{sh}$ and $\Delta\varepsilon_{rs}^{T}$ are the strain increments for shrinkage and thermal strains, $\Delta\sigma_{ij}^{cr}$ is the stress increments for cracked part, $\Delta\sigma_{ij}''$ is the inelastic strain increment, C_{ijrs} is the stiffness tensor that can be evaluated as

$$C_{ijrs} = \frac{3\pi}{2}\int [n_i n_j n_r n_s C_D + \frac{1}{3} n_i n_j \delta_{rs}(C_V - C_D)]F(n)dS \tag{19}$$

$$\Delta\sigma_{ij}'' = \frac{3\pi}{2}\int_S n_i n_j (\Delta\sigma_V'' + \Delta\sigma_D'')F(n)dS \tag{20}$$

$$\Delta\sigma_{ij}^{cr} = C_{ijrs}\Delta\varepsilon_{rs}^{cr} \tag{21}$$

$$\Delta\varepsilon_{rs}^{cr} = n_r n_s \varepsilon_{cri} \tag{22}$$

where C_V and C_D are the incremental volumetric and deviatoric secant moduli for current loading for a microplane. $\Delta\sigma_V''$ and $\Delta\sigma_D''$are the inelastic volumetric and deviatoric stress increments. $\Delta\varepsilon_{rs}^{cr}$ is the strain increments for cracked part. (F(n) = 1 which is a weight function of the normal direction that can introduce anisotropy in its initial state). n with subscripts i,j,r,s are the direction cosines.

$$C_V = C_V^{\circ}(1 - \omega_V) \qquad C_D = C_D^{\circ}(1 - \omega_D) \tag{23}$$

$$\varepsilon_V < 0 \qquad C_V = C_V^{o}\left[\left(1 + \left| \frac{\varepsilon_V}{a} \right| \right)^{-m} + \left| \frac{\varepsilon_V}{b} \right|^{q} \right] \tag{24}$$

$$\varepsilon_v \geq 0 \qquad \omega_V = 1 - \exp\left[-\left(\frac{\varepsilon_V}{e_1} \right)^{l} \right] \tag{25}$$

$$\varepsilon_D \geq 0 \qquad \omega_D = 1 - \exp\left[-\left(\frac{\varepsilon_D}{e_1} \right)^{l} \right] \tag{26}$$

$$\varepsilon_D < 0 \qquad \omega_D = 1 - \exp\left[-\left(\frac{\varepsilon_D}{e_1} \right)^{n} \right] \tag{27}$$

where e_1, l, n, a, b, m, q are the material empirical constants and C_V°, C_D° are the initial volumetric and deviatoric secant moduli, ω_V, ω_D are volumetric and deviatoric damage coefficients and ε_V, ε_D are the volumetric and deviatoric strains respectively.

2.5 Crack distribution model

The crack distribution of SHCC can be modelled by assuming uniform discrete distribution of fibers. The cracking sequence can be explained based on various experimental data. The first crack will appear at the middle specimen with least fiber volume/tensile strength. The subsequent cracks will appear in the middle of each equally spaced section from left to right with statistically increasing fiber volume at each discrete interval (see Fig.7). This process continues till crack spacing will equal to critical crack spacing. At this stage localization of cracks will start.

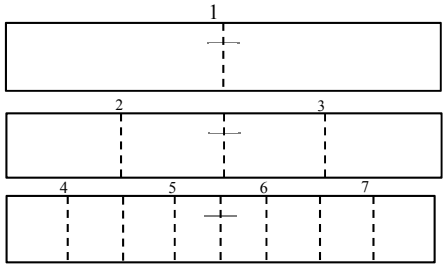

Fig 7 Crack distribution/spacing model for SHCC

3. RESULTS AND DISCUSSIONS

3.1 Uniaxial tensile loading

To demonstrate the capability of present multi-layered microplane model in predicting the uniaxial tensile stress-strain behavior, the analytical verification for SHCC is carried out and this is done by comparing results with experimental work [6]. The matrix and fiber properties are given in Table 1.

For computation, the simplified form of microplane model [9] is followed with certain assumptions. The strain hardening cementitious composites show almost negligible shear resistance as synthetic fibers are very flexible. Hence for present model, practically the resistance in tangential direction is neglected i.e. $C_T = 0$. Another simplification is made by considering normal stiffness equal to volumetric stiffness (deviatoric stiffness is assumed to be negligible), i.e., $C_N = C_V$ and $C_D = 0$. Further, the normal stiffness is used as tangent modulus in normal direction. Therefore, considering E_N equal to initial modulus, the expression for tangent modulus can be obtained as $C_N^T = E_N e^{-k\varepsilon_N{}^p}(1 - kp\varepsilon_N{}^p)$ where k (softening parameter)and p are material constants and $\varepsilon_V = \varepsilon_N$. These parameters can be related to parameters used for secant modulus in Eq. 25 as $(1/e_1)^l = k$, $l = p$, $C_V^0 = E_N$ The value of two elastic constants, Poisson's ratio ν and initial modulus E_N are fixed prior to data fitting. The total macroscopic strain is considered as sum of strain due to microplane system e_{ij} and additional elastic strain ε_{ij}^a, i.e., $\varepsilon_{ij} = e_{ij} + \varepsilon_{ij}^a$. The related detail of derivation of ε_{ij}^a and definition and value of parameters are given in Ref. [10].

The comparison results of analytical and experimental data have been depicted in Fig.8. The computation is done for two different behaviors, i.e., by SL (single layer) model and ML (multi-layered) model for SHCC where former model represents the overall behavior as single layer of microplane model and latter represents the overall behavior as multi-layered microplane model that is obtained by the envelope of each SLC (single layer at each crack) model behavior. There is some difference of behavior is observed in SL model results because the exponential variation of tangent stiffness is considered in this model while in real behavior the stiffness of SHCC does not vary exponentially. In data fitting, much focus has been given to adjust maximum tensile strength and strain-hardening up to certain extend. This comparison is modified by using ML model in which not only the initial stiffness but strain-hardening and multiple cracking of SHCC is also verified. The simplification is made by considering tensile strength varying from minimum to maximum tensile strength from test data. The material parameters for SL and SLC model are given in Table 2. The value of k is variable for each SLC model, i.e., 30000, 27000, 26000, 25000, 24000, 23000, 22500, 22000, 21800, 21500, 21000, 20500, 20000 from 1st SLC model to 12th SLC model.

3.2 Total crack width and crack distribution

This model can efficiently be used to simulate total crack width at increasing load steps. The simulation results are verified by comparing with experimental data [6]. In this work, the average crack widths are measured at 0.5%, 1% and 2% strain values with 4, 8 and 12 number of cracks respectively at corresponding strain values. The total crack width can be evaluated by multiplying the crack width with number of cracks and considering standard deviation value for crack width given in the experimental data. The fiber and matrix properties are given in Table 1. For simulation of total crack width, Eq.15 is used.

For this purpose, tensile strength/loads are taken from the experimental data of uniaxial tensile stress-strain relationship at each crack [6]. The mean volume fraction is considered as 2.25%. The uniform distribution of fiber volume fraction is considered from 1st crack (minimum) to 12th crack (maximum).

The standard deviation value is considered as 0.11%. Hence considering equally spaced cracks, the values of volume fraction from 1st crack to 12th crack are calculated as 1.68%, 1.8%, 1.9%, 2.02%, 2.13%, 2.25%, 2.36%, 2.47%, 2.58% 2.7% 2.81% and 2.92%. The total cross sectional areas of bridging fibers are calculated corresponding to above fiber volume fractions at each crack. The stiffness of bridging fibers is calculated as $k_f = E_f A_{fi}/L$ where L is the debonding length of bridging fiber that is considered as $L_f/2$ in this case where L_f is the length of fiber. The E_f is the elastic modulus of fibers that is considered constant and adjusted by the first crack width of measured data, i.e. , E_f = 4740 MPa. The simulation results are shown in Fig.9 which shows satisfactory agreement with

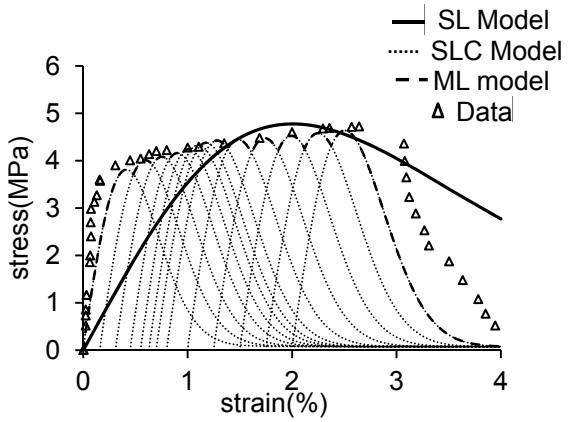

Fig.8 Comparison of analytical results with test data for uniaxial tension of SHCC [6]

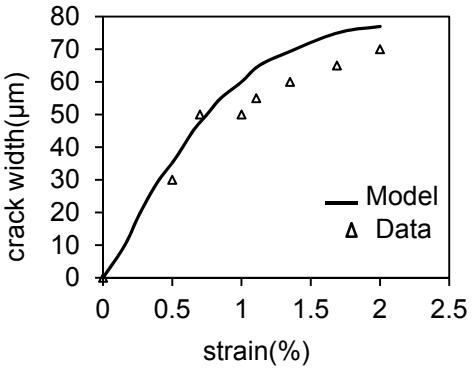

Fig.9 Comparison of analytical results with test data for total crack width of SHCC [6]

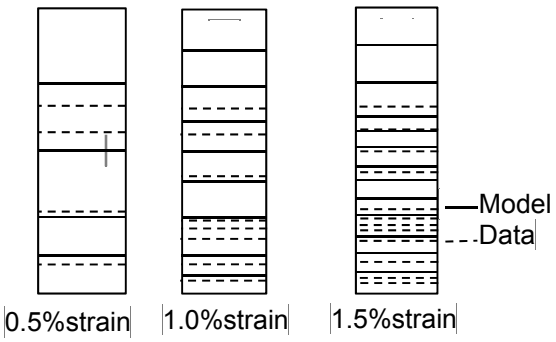

Fig.10 Comparison of model results with test data for crack distribution/spacing of SHCC [6]

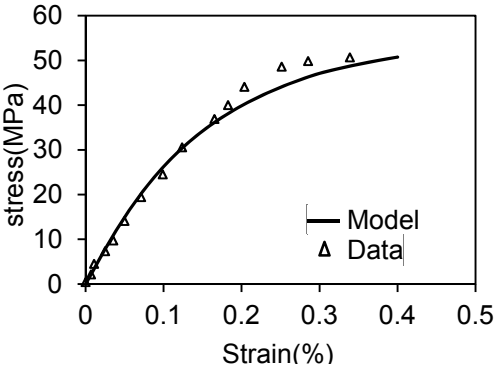

Fig.11 Comparison of analytical results with test data for uniaxail compression of SHCC [7]

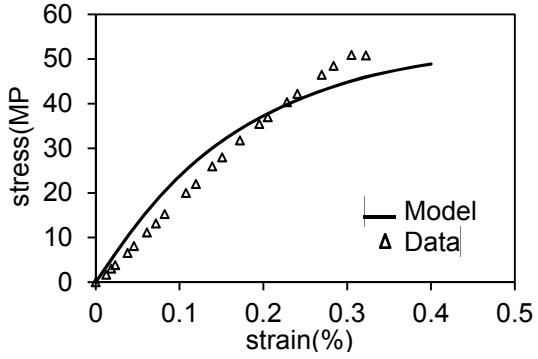

Fig.12 Comparison of analytical results with test data for uniaxial compression of SHCC [8]

Table 1 Fiber and matrix properties

Properties	Uniaxial tensile loading/ Total crack width [6]
Specimen size (mm)	100x40x24
Fiber volume (%)	2.25
Fiber length (mm)	12
Fiber diameter (μm)	40
Stress at first cracking (MPa)	3.6
Tensile strength (MPa)	4.7

Table 2 Material parameters for analytical verification of material behavior

Model Param-eters	Uniaxial tension SLC [6]	Uniaxial tension SL [6]	Uniaxial compression [7]	Uniaxial compression [8]
E_N (MPa)	4500	1100	35000	30000
ν	0.2	0.2	0.20	0.2
k	-	1100	0.0	0.0
d	0.0	0.0	39	38
p	0.20	0.20	0.20	0.20

Table 3 Fiber and matrix properties

Properties	Uniaxial compression [7]	Uniaxial compression [8]
Fiber volume (%)	2.0	2.0
Fiber length(mm)	38	12
Fiber diameter(μm)	38	39
Peak stress(MPa)	49.9	51
Peak strain (%)	0.27	0.32

experimental data.

3.3 Crack distribution/spacing

To model crack distribution and number of cracks, the data [6] is referred. In this case total of 12 cracks are observed during strain-hardening zone. The crack distribution by experimental results may be attributed to non-uniform distribution of mechanical properties. This whole range is divided uniformly into 12 discrete statistical intervals. The first crack will appear at the middle of the first statistical interval and this sequence will continue from left to right. The verification results are shown in Fig.10 which depicts a satisfactory agreement with experimental data of crack distribution at 0.5%, 1.0% and 2.0% strain values. It is clear from figure that at 0.5% strain, number of cracks is four, at 1.0% strain number of cracks is eight and at 2.0% strain number of cracks is twelve which verify the experimental results for number of cracks based on uniform statistical increase of fiber volume.

3.4 Uniaxial compression

The presented microplane model can also be implemented for simulating uniaxial compression behavior. The analytical results are compared for two different experimental data by Refs. [7] and [8]. The related fiber and material properties are given in Table.3. For uniaxial compression, the assumptions are considered, i.e., $C_V = C_N$, $\varepsilon_V = \varepsilon_N$, $C_D = 0$ and $C_T = 0$ .The tangent modulus is calculated as arctan function as $C_N^T = E_N/(1+(\omega\varepsilon_N)^2)$ where $\omega = \pi E_N / 2d$ in which d is compressive strength parameter. The elastic material constants E_N (initial modulus) and Poisson's ratio ν are fixed and then d is identified by computation. The adjusted value of material parameters are shown in Table 2. The analytical results show satisfactory agreement with experimental data as shown in Figs.11-12.

4. CONCLUDING REMARKS

(1) The results show the applicability of multi-layered microplane model with good agreement with experimental data. This model has an advantage of predicting total crack width, crack distribution/spacing and number of cracks. In this way the phenomenon of multiple cracking and stress-strain relationship for uniaxial tensile loading can be predicted. This model is comparatively more realistic to state crack distribution behavior of SHCC.

(2) The multi-layered microplane model has wide range of applicability. This can be implemented for various strengths of the SHCC material and fiber volume. The material behavior can be simulated for a wide range of tensile or compressive strengths and fiber volume as fiber volume is observed the main parameter that identifies the SHCC material behavior.

(3) Being three dimensional analytical characteristics, this model can be extended to multi-axial loading of strain-hardening cementitious composites along with uniaxial behavior. Various experimental data is available for biaxial and triaxial compressive behavior [7] and [8]. This can contribute an efficient advantage of this model. The model details and analytical verifications will appear in continuation of recent research work.

REFRENCES

[1] Mechtcherine, V., Schulze, J., "Behavior of strain hardening cementitious composites in tension", International RILEM workshop on high performance fiber-reinforced composites in structural applications PRO 49, 2006, pp.37-46.

[2] Han T.S., Feenstra P.H., Billington S.L., "Simulation of highly ductile fiber reinforced cement-based composite components under cyclic loading", ACI Structure Journal, 100(6), 2003, pp.749-757.

[3] Vorel J., Boshoff W.P., "Numerical modelling of strain hardening fiber-reinforced composites", International conference on advanced concrete materials, ACM 2009, Stellenbosch, South Africa, Vol 100, pp. 271-278.

[4] Ozbolt J. and Bazant Z. P. , "Microplane model for cyclic triaxial behavior of concrete", J. of Eng. Mech., Vol. 118 No.7, 1992, pp.1365-1386.

[5] Kabele P. and Horii H., "Analytical model for fracture behaviors of pseudo strain-hardening cementitious composites", J. Materials Concrete Structural Pavements, No.532/V-3, 1996, pp.209-219.

[6] Jun P., Mechtcherine V., "Behavior of strain-hardening cement-based composites (SHCC) under monotonic and cyclic tensile loading. Part 1-Experimental investigations", Cement and concrete composites, Vol 32, 2010, pp. 801-809.

[7] Sirijaroonchai K., Tawil S.E., Parra-Monstesinos G., "Behavior of high performance fiber reinforced cement composites under multi-axial compressive loading", Cement and concrete composites, Vol 32, 2010, pp.62-72.

[8] Zhou J.J, Pan J.L, Leung C.K.Y. and Li Z.J., "Experimental study on mechanical behaviors of pseudo-ductile cementitious composites and normal concrete under biaxial compression", VIII international conference on FraMCos-8, 2013, pp. 963-969.

[9] Bazant Z.P., and Prat P.C., "Microplane model for brittle-plastic material: I Theory", Journal of Engineering Mechanics, ASCE, Vol.114, No. 10, 1988 , pp.1672-1687.

[10] Bazant Z.P., and Gamnarova P.G., "Crack shear in concrete: Crack band microplane model", Journal of Structural Engineering, Vol.110, 1984, pp.2015-2035.